JOURNAL OF GEOPHYSICAL RESEARCH, VOL. 115, C01005, doi:10.1029/2008JC005189, 2010

A stochastic formulation for erosion of cohesive sediments

B. C. Van Prooijen[1] and J. C. Winterwerp[2]

Received 10 November 2008; revised 9 September 2009; accepted 17 September 2009; published 15 January 2010.

[1] The linear formulation for erosion $E = M(\tau_b - \tau_c)$, often applied in engineering applications, has two properties, which do not always comply with field and laboratory observations, they are as follows: (1) The erosion rate is zero below the critical bed shear stress τ_c and increases linearly with bed shear stress τ_b, when exceeding the critical bed shear stress; incipient motion ($\tau_b \simeq \tau_c$) is poorly represented. (2) The erosion rate is constant in time for constant values of M and τ_c, whereas observations often suggest time dependency. In this paper we analyze the process of incipient motion and time dependency by using a stochastic forcing (bed shear stress) and a stochastic bed strength (critical bed shear stress). It is well known that the bed shear stress is not constant but varies due to turbulence. This stochastic nature of the turbulent motion is accounted for by a probability density distribution for the bed shear stress, which is based on the formulation of Hofland and Battjes (2006). This distribution is implemented in the linear erosion formulation. An analytical solution for the erosion rate is obtained, which only depends on the mean bed shear stress. A parametrization is made for efficient application in numerical models. The sediment in the bed is considered to be nonuniform. Therefore, it is subdivided into several classes, distinguished by the critical bed shear stress and not necessarily by the grain size. The variability of the critical bed shear stress is treated in a discritized way. Sediment balance equations are solved for each class. Considering different classes, the total erosion rate becomes time dependent, as the erosion depends on the availability of sediment. The model is applied to two annular flume data sets, Jacobs (2009) and Amos et al. (1992a). The results show that with a proper choice of the required parameters, the time dependence of the erosion rate and the concentration can be reproduced. We conclude that the occurrence of incipient motion can be explained from a stochastic forcing. Time-varying erosion rates can be explained from a stochastic bed strength distribution or from a vertical gradient in bed strength. The latter is, however, not likely and not measurable in the top layers of dense consolidated cohesive sediment beds.

Citation: Van Prooijen, B. C., and J. C. Winterwerp (2010), A stochastic formulation for erosion of cohesive sediments, *J. Geophys. Res.*, *115*, C01005, doi:10.1029/2008JC005189.

1. Introduction

[2] Fine (cohesive) sediments play a key role in aquatic ecosystems as these sediments in suspension determine light penetration into the water column; hence affect primary production; determine the strata of the seabed supporting benthic life; and the sediment's organic content forms food supply to filter feeders. Therefore, the behavior of fine sediments often forms a central theme in assessing the impact of infrastructure and management strategies. Such assessments often require the use of numerical fine sediment transport models, as the relevant processes are too complicated to be resolved with analytical tools. Because the ecosystems addressed are shallow, water bed exchange processes, i.e., erosion and deposition, determine the transport and the fate of fine sediments. In the past decades biological effects on erosion have been shown to be of major importance, see *Le Hir et al.* [2007] for a recent overview. Erosion can be enhanced by biodestabilizers and reduced by biostabilizers. Furthermore, organisms can mix the seabed. In this paper biological effects are not directly accounted for, but the proposed framework offers several possibilities to implement biological influences. This is for example shown for the effect of Macoma balthica on erosion shown by *Van Prooijen and Montserrat* [2009]. We will focus here on the erosion of fine sediments by flow-induced currents.

[3] Various devices have been developed to determine the erosion rate by flow: carousels [*Parchure and Mehta*, 1985; *Kuijper et al.*, 1989; *Amos et al.*, 1992b], straight flumes [*Partheniades*, 1965; *Aberle et al.*, 2003; *Le Hir et al.*, 2005; *Roberts et al.*, 1998; *Orvain et al.*, 2003], portable annular flumes [*Willows et al.*, 1998; *Widdows et al.*, 1998], and vertical jet devices [*Tolhurst et al.*, 1999]. Various mud beds have been studied: deposited beds, placed beds, and natural beds. Measurements have been carried out in laboratories as

[1]Hydraulic Engineering Section, Department of Civil Engineering, Delft University of Technology, Delft, Netherlands.
[2]Environmental Fluid Mechanics Section, Department of Civil Engineering, Delft University of Technology, Delft, Netherlands.

0148-0227/10/2008JC005189$09.00

well as in the field. A major finding of these experiments is the existence of a threshold, the so-called critical bed shear stress for erosion τ_c, beyond which significant erosion is observed. From laboratory studies, *Mehta and Partheniades* [1982] identified two main types of erosion, referred to as Type I and Type II erosion.

[4] Type I describes erosion rates decreasing in time at constant forcing. This behavior is explained by a critical bed shear stress, which increases with depth, i.e., the bed is stratified. At the depth where the bed shear stress equals the critical bed shear stress, erosion stops. This type of erosion is therefore also called depth-limited or supply-limited erosion. *Mehta and Partheniades* [1982] established such stratification for fluffy, deposited beds with bulk densities of ρ_b = 1100–1300 kg m^{-3}, by measuring vertical density profiles. In more dense beds, with bulk densities of approximately ρ_b = 1800 kg m^{-3} like those given by *Amos et al.* [1992a], these density profiles could not be measured as the eroded layer was less than 1 mm thick. *Amos et al.* [1992a] made a further distinction between Type Ia and Type Ib erosion. Type Ia occurs at relatively low forcing and is associated with faecal pellets produced by the amphipod *Corophium volutator*. Type Ib erosion occurs at higher bed shear stresses (1.0–4.4 Pa [*Amos et al.*, 1992a]). In case of uniform strength of the bed over the depth, the erosion rate remains constant in time at constant forcing. This type of erosion is called Type II erosion, or unlimited erosion. As shown by *Amos et al.* [1992a], this type of erosion occurred for shear stresses of 2–10 Pa. This distinction between Type I and Type II erosion has been found in many laboratory and field studies.

[5] Various erosion rate formulations have been developed to describe Type I and Type II erosion. For Type I, a formulation for the erosion rate of the form $E = E_0 \exp(-\lambda t)$ often fits the data well [e.g., *Maa et al.*, 1998], implying that in the long run, erosion rates reduce to zero. For Type II erosion, an exponential form was proposed for freshly deposited beds by *Mehta and Partheniades* [1982], $E/\epsilon_0 = \exp[\alpha(\tau_b/\tau_c - 1)^n]$, with coefficients ϵ_0, α and n. Most often the linear relation $E = M(\tau_b/\tau_c - 1)$ is applied, first proposed by *Kandiah* [1974], although the measurements of *Partheniades* [1965] already suggested such a relation. The linear relation has been generalized by others through a power law relation, $E = M(\tau_b/\tau_c - 1)^n$. *Sanford and Maa* [2001] derived a unified erosion formulation by using the linear formulation and by defining M and τ_c variable over depth. With this formulation, Type I and Type II erosion can be simulated. Erosion stops when a critical bed shear stress is reached which equals the bed shear stress (Type I erosion). Unlimited erosion (Type II) is possible for beds for which the critical bed shear stress is always smaller than the imposed bed shear stress.

[6] The linear formulation with constant values for M and τ_c is most often applied in numerical studies [see, e.g., *Pritchard and Hogg*, 2003; *Van Ledden et al.*, 2004; *Stanev et al.*, 2007]. This formulation is characterized by a threshold bed shear stress above which significant erosion rates are predicted. However, some erosion takes place below this critical bed shear stress. Therefore, the erosion rate at these small bed shear stresses is actually not zero. This so-called incipient motion can be explained in the following two ways: (1) The eroding force, i.e., the turbulent flow, is stochastic by nature; hence, the bed strength will almost always be exceeded by peak stresses and erosion will occur. (2) The bed properties are nonuniform in horizontal space; therefore, some parts of the sediment beds are more likely to erode than others, due to, e.g., difference in particle size, difference in cohesive bonding, or exposure to the flow. This incipient motion is important for the modeling of sediment transport for the following two reasons: (1) Even small rates of erosion may mobilize large amounts of fine sediments affecting the ecosystem. (2) From the mathematical point of view, the linear erosion formulae may yield unfavorable model behavior, in particular when gradients in, e.g., bed shear stress and/or bathymetry are large. Improving the formulations for incipient motion is therefore desirable.

[7] In this paper we elaborate on the stochastic behavior of the eroding force and on the nonuniformity of the critical bed shear stress, quantifying incipient motion and accounting for supply-limited and -unlimited erosion. Our overall objective is to enhance our understanding on the role of stochastic processes on the erosion of cohesive beds. In section 2 we give a background on previous work on stochastic erosion rate formulations. A probability density function (PDF) of the bed shear stress is derived in section 3. This PDF is implemented in the linear erosion formulation in section 4. A stochastic description of the critical bed shear stress is given in section 5. In sections 6 and 7 the new formulation with stochastic forcing and variable critical bed shear stress is applied to simulate the results of experiments in annular flumes. The paper finishes with a discussion and conclusions in section 8.

2. Background: Stochastic Erosion Formulation

[8] The linear erosion rate formulation is defined by $E = M(\tau_b - \tau_c)$ for $\tau_b > \tau_c$. This formulation is often ascribed to Partheniades. However, he was not the one who used this formulation for the first time. According to *Krone* [1999], we have to cite *Kandiah*'s [1974] relation to refer to the linear formulation. (The linear formulation is suggested to be referred to as the Ariaturai-Partheniades equation according to *McAnally and Mehta* [2001]. However, *Krone* [1999] specifically refers to "Kandiah's relation." As he was the promotor of both Kandiah and Ariathurai, we follow his reference. Note however that Kandiah used the "dimensionless" form $E = M(\tau_b/\tau_c - 1)$, whereas Ariathurai used the form form $E = M(\tau_b - \tau_c)$.) Note that from a dimensional point of view, a formulation of the form $E = M(\tau_b/\tau_c - 1)$ seems more plausible. However, when such a formula is used to fit experimental data, large errors can emerge near the onset of erosion (when $\tau_b \sim \tau_c$). Therefore we advocate the use of $E = M(\tau_b - \tau_c)$.

[9] The critical bed shear stress for erosion τ_c is obtained by fitting the linear erosion formulation $E = M(\tau_b - \tau_c)$ through experimental data. Thus, by definition, τ_c is the bed shear stress at which the linear formulation crosses the τ_b axis. This implies that the linear formulation for erosion has the following two properties, which often do not comply with reality: (1) The erosion rate is zero below the critical bed shear stress and increases linearly for shear stresses exceeding the critical bed shear stress. (2) The erosion is constant in

time for constant values of M and τ_c, whereas experiments and surveys often suggest a time dependence. Both aspects are discussed in this section.

[10] Nonzero erosion rates at $\tau_b < \tau_c$ are clearly observed in experiments by for instance *Partheniades* [1965]. Small erosion rates can be of importance for the development of mud beds. A relation taking into account these small rates is therefore desired. *Partheniades* [1965] was the first to formulate an analytical expression for the erosion of cohesive sediment. He took into account the probability density distribution (PDF) of the bed shear stress in his erosion rate formulation. As we will follow a similar procedure, we briefly discuss his derivation.

[11] *Partheniades* [1965] defined the erosion rate E [kg m^{-2} s^{-1}] as

$$E = \frac{AD_s\gamma_s}{t^{\tau_b}} P\left\{\frac{k\tau_b}{c} \geq 1\right\}, \quad (1)$$

with shape factor A, typical particle/cluster diameter D_s, unit weight $\gamma_s = \rho_s - \rho_w$ (with solid density ρ_s and water density ρ_w), time scale for breaking particles from the bed t^{τ_b} (*Partheniades and Paaswell* [1970] refer to the time scale t^{τ_b} as "... time required for a stress $k\tau_b/c > 0$ to act for the removal of a particle..."), bed shear stress τ_b, proportionality factor k, macroscopic shear strength c, and $P\{\}$ the probability that the expression between brackets is fulfilled. The probability P varies between 0 and 1. Equation (1) is identical to the formulation proposed by *Einstein* [1950], derived for bed load of noncohesive sediment. A normal distribution for the bed shear stress was assumed by Partheniades. The parameters A, k, c and t^{τ_b} were calibrated against the results of his flume experiments. No information is given on how the time scale t^{τ_b} relates to the bed shear stress τ_b, nor are the values of the other parameters given. However, if t^{τ_b} is a function of τ_b, t^{τ_b} should be within the probability P. This will be explained further in section 4. Since the publication of *Partheniades* [1965], the knowledge on turbulent boundary layers has improved from detailed measurements and direct numerical simulations (DNS). The PDF of the bed shear stress is known in more detail, see measurements of *Obi et al.* [1996] and *Miyagi et al.* [2000] and DNS results of *Kim et al.* [1987]. *Hofland and Battjes* [2006] derived a more physically sound description of the PDF of bed shear stresses.

[12] The erosion rate of cohesive sediment is often time dependent at constant forcing, as shown in literature mentioned. The erosion rate generally increases rapidly to a peak value and then becomes constant, or even zero. Several explanations are possible for this time-dependent behavior [see, e.g., *Lick*, 2009] (1) erosion balances deposition, (2) erosion decreases with eroded depth (mass), and (3) the sediment consists of nonuniform material.

[13] The first hypothesis was falsified by *Parchure and Mehta* [1985] for fine cohesive sediments. They carried out an erosion experiment in an annular flume. When equilibrium (i.e., no net erosion) was attained, they gradually replaced the sediment-laden water with clean water. If deposition would have played a role, further erosion should have taken place. However, no further erosion was detected. The concentration in the water decreased exponentially, according to the decay expected from the replacement of suspension with clean water.

[14] The second hypothesis was proposed by *Mehta and Partheniades* [1982] and adopted by *Parchure and Mehta* [1985], *Amos et al.* [1992a], and *Sanford and Maa* [2001]. This concept is applied in a bed model by *Sanford* [2008]. In the case of a bed created from deposition [e.g., *Parchure and Mehta*, 1985] with $\rho_b = 1100-1300$ kg m^{-3}, the bulk density increases with depth. The critical bed shear stress is therefore expected to increase with depth as well. The depth over which this gradient was found is of the order of several centimeters. In case of denser beds, as observed in the field [e.g., *Amos et al.*, 1992a] $\rho_b \approx 1800$ kg m^{-3}, the thickness over which this gradient was found, is of the order of 0.01–0.3 mm. As density measurements are not possible in such thin layers, it is not possible to validate the second hypothesis directly for dense beds. *Amos et al.* [1992a] also showed typical diameters of eroded aggregates, though they did not mention how these aggregates were measured, and if these were averaged values. However, the diameters, ranging from 2–7 mm, are significantly larger than the averaged thickness of the eroded layer. For the relatively dense beds, it is difficult to match the thin layer, over which the shear stress increases, with the large sizes of the aggregates.

[15] The third hypothesis for the time variation of the erosion rate assumes a nonuniform critical bed shear stress. At a given forcing, sediment particles with an erosion threshold smaller than the forcing will erode, whereas the particles with a larger threshold will remain in the bed. When all sediment with thresholds lower than the eroding forcing is eroded, erosion stops. This picture is comparable to armoring found in river systems with sand and gravel. Mud beds consist of flocs, which are different in size and may be attached to other flocs by different cohesion (and/or adhesion) forces. In case of natural mud, the sediment consists of clay, silt and sand, resulting in a nonuniform erosion threshold. Another possible reason for a nonuniform erosion threshold is the presence of bed irregularities or ripples. The top of the ripples and other protruding elements are more exposed and will erode more easily. Flattening of the irregularities results in a smoother surface, implying smaller erosion rates.

[16] To the authors' knowledge, the third hypothesis has not been explored yet with respect to the erosion of fine cohesive sediments. It is however widely assumed in the modeling of noncohesive nonuniform sediment, see, e.g., *Wiberg et al.* [1994] for continental shelves or *Blom* [2003] for river systems. Note that the three phenomena, as discussed above, may exist simultaneously. This paper discusses only nonuniformity in erosion characteristics of the sediment and we neglect the effects of deposition (Hypothesis 1) and stratification (Hypothesis 2).

3. Bed Shear Stress Distribution

[17] The probability density function of the bed shear stress (τ_b) is based on the derivation of *Hofland and Battjes* [2006]. The following assumptions were made: (1) The mean bed shear stress is proportional to the friction velocity squared, $\langle\tau_b\rangle = \rho_w\, u_*|u_*|$, with bed shear stress τ_b and water density ρ_w. (2) A fictive near bed velocity u_b is defined such that its root mean square equals the friction velocity,

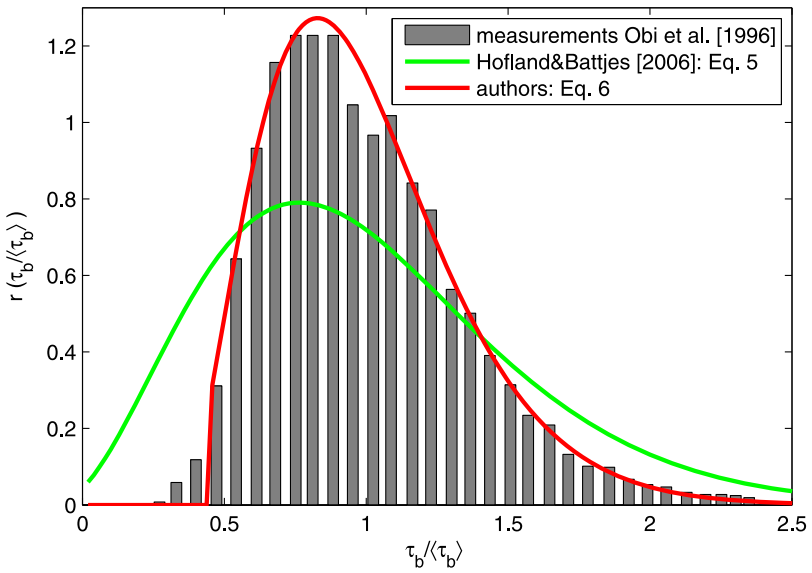

Figure 1. Measurements of bed shear stress normalized by the mean bed shear stress (from *Obi et al.* [1996]), the relation of *Hofland and Battjes*'s [2006] equation (5), and the authors' modified relation (equation (6)).

$u_*^2 = \mu_u^2 + \sigma_u^2$. The near-bed velocity u_b has a Gaussian distribution with mean value μ_u and standard deviation σ_u. The following dimensionless parameters are introduced:

$$\omega = \frac{u_b}{\sigma_u}; \qquad \delta = \frac{\mu_u}{\sigma_u}; \qquad T_b = \frac{\tau_b}{\rho_w \sigma_u^2} = \omega|\omega|, \tag{2}$$

with ω the dimensionless near-bed velocity, δ the dimensionless mean velocity and T_b the dimensionless bed shear stress. All parameters are scaled with the standard deviation σ_u of the near-bed velocity. Such a scaling is similar to a scaling with u_* as $\sigma_u = \sqrt{1+\delta^2}u_*$. The Gaussian distribution $q(\omega)$ for the scaled near-bed velocity ω reads

$$q(\omega) = \frac{1}{\sqrt{2\pi}} \exp\left[-\frac{1}{2}(\omega - \delta)^2\right]. \tag{3}$$

Following *Hofland and Battjes* [2006], the distribution of the bed shear stress is defined by

$$r(T_b) = q(\omega)\frac{\mathrm{d}\omega}{\mathrm{d}T_b} = q(\omega)\frac{1}{2\sqrt{T_b}}. \tag{4}$$

In this paper we only consider uniform open channel flow. In this type of flow, the negative bed shear stresses (i.e., in opposite flow direction) are negligible, see Figure 1. The distribution of the bed shear stress then reads

$$r(T_b) = \frac{1}{2\sqrt{2\pi T_b}} \exp\left[-\frac{1}{2}\left(\sqrt{T_b} - \delta\right)^2\right]. \tag{5}$$

Only the parameter δ has to be determined to obtain the distribution of the bed shear stress. This parameter is calibrated by *Hofland and Battjes* [2006], using the measurements of *Obi et al.* [1996], resulting in $\delta = 3.5$. This value gives a good approximation for the shape of the distribution. The measured skewness and flatness factors from *Obi et al.* [1996] are $SF = 0.95$ and $FF = 4.56$, respectively. The modeled factors with $\delta = 3.5$ are in fair agreement, $SF = 0.84$ and $FF = 3.94$. However, significantly different is the ratio of the standard deviation to the mean value. The measured ratio is $\tau'_b/\langle\tau_b\rangle = 0.35$, whereas the modeled distribution gives a value of $\tau'_b/\langle\tau_b\rangle = 0.54$. This discrepancy is probably overlooked by *Hofland and Battjes* [2006] as they plotted the distribution against $(\tau_b - \langle\tau_b\rangle)/\tau'_b$. Figure 1 shows the measured distribution and the distribution according to equation (5) with $\delta = 3.5$ against $\tau_b/\langle\tau_b\rangle$.

[18] The measured ratio of $\tau'_b/\langle\tau_b\rangle = 0.35$ could not be obtained by changing δ only, as skewness and flatness will deviate then as well. Obi's measurements can only be matched by changing the standard deviation of the distribution by multiplying the scaled bed shear stress T_b by a factor (α). This change must then be compensated for to obtain the correct mean bed shear stress, $\langle\tau_b\rangle = \rho u_*^2$. This compensation is assumed to be proportional to $\mu_u^2/\sigma_u^2 = \delta^2$. Then, the resulting formulation for the bed shear stress distribution becomes

$$r(T_b) = \frac{\alpha}{2\sqrt{2\pi T_b^*}} \exp\left[-\frac{1}{2}\left(\sqrt{T_b^*} - \delta\right)^2\right], \tag{6}$$

with $T_b{}^* = \alpha T_b - \beta\delta^2$.

[19] The parameters α, β and δ are fitted to match the data of *Obi et al.* [1996]. With δ the skewness and flatness can be tuned. A value of $\delta = 3.1$ gave skewness factor $SF = 0.93$ and flatness factor $FF = 4.2$. The measured values are $SF = 0.95$ and $FF = 4.56$. The ratio between the standard deviation and the mean value $\tau'_b/\langle\tau_b\rangle = 0.35$ is determined by the parameter α $\alpha = 1.75$. To obtain the proper mean value of $\langle\tau_b\rangle = \rho u_*^2$, we set set $\beta = 0.83$. The resulting distribution is given in Figure 1. Note that the bed shear stress is scaled with its mean value and not with the standard deviation.

[20] The Reynolds number of the experiment of *Obi et al.* [1996] was relatively low, Re = 6600, and the bed was smooth. Other experiments mentioned by *Obi et al.* [1996] give the following ranges: $\tau'_b/\langle\tau_b\rangle$ = 0.35–0.40, SF = 0.8–1.1 and FF = 4.0–4.8. The data of *Miyagi et al.* [2000], Re = 17,400–35,000 give $\tau'_b/\langle\tau_b\rangle$ = 0.4, SF = 1.09 and FF = 4.6. For even higher Reynolds numbers and for rough beds, as found in the field, no sound measurements of the PDF of the bed shear stress are found. Only some values for $\tau'_b/\langle\tau_b\rangle$ are available:; *Einstein* [1950] uses 0.36 and *De Ruiter* [1982] uses 0.4. Wind tunnel experiments were carried out for high Reynolds number flows (Re = 0.6–2.1 10^6) by *Ruedi et al.* [2004]. They found that the skewness and flatness are Reynolds number dependent. However, they consider this as a measurement error and they expect a constant skewness and flatness over the range they considered. In this paper, we only consider uniform channel flow. In case of acceleration and deceleration, other values for δ are expected [see *Hofland and Battjes*, 2006]. Given the available data, we conclude that the presented PDF is valid for steady uniform flows with Reynolds numbers up to 35,000 and a smooth bed. But, we could not find indications that the PDF would not be valid for flows with higher Reynolds numbers, rough beds and nearly uniform conditions as found in nature on, e.g., tidal flats.

[21] Note that the formulation of equation (6) tends to infinity when $T_b^* = \alpha T_b - \beta\delta^2$ approaches zero. As mentioned, this range of bed shear stresses, which is the left tail of the distribution, is however of negligible importance within the context of the present study, as this part of the distribution will hardly contribute to erosion.

[22] To summarize, a good approximation for the distribution of the bed shear stress is obtained, but no physical reason is found for the required scaling of the formulation of *Hofland and Battjes* [2006]. In-depth research is needed in future to support this adaptation to reproduce the measured bed shear stress distribution.

4. Implementation of $r(T_b)$ in the Linear Erosion Rate Formulation

[23] The erosion rate of mud is generally expressed by the linear formulation $E = M(\tau_b - \tau_c)$ for $\tau_b > \tau_c$, with a mean value for the bed shear stress τ_b and a constant value for the critical bed shear stress τ_c. This relation mainly holds for bed shear stresses much larger than the critical bed shear stress. For bed shear stresses of the order of the critical bed shear stress, this formulation deviates from measurements [see *Partheniades*, 1965]. Note that the results of *Partheniades* [1965] are obtained by sequentially increasing the eroding velocity in steps, where each step lasted several 10s of hours. They can therefore be considered as Type II erosion.

[24] In case of a distribution of bed shear stresses, the erosion rate dE for the bed shear stress $\tau_{b1} < \tau_b < \tau_{b2}$ becomes

$$\mathrm{d}E = \mathrm{d}\tau_b r\{\tau_b\} M(\tau_b - \tau_c), \tag{7}$$

with $\mathrm{d}\tau = \tau_{b2} - \tau_{b1}$ and $r\{\tau_b\}$ the probability that $\tau_{b1} < \tau_b < \tau_{b2}$. To determine the total erosion rate, we integrate equation (7) from $\tau_b = \tau_c$ to $\tau_b \rightarrow \infty$. Note that all bed shear stresses are positive by virtue of the assumed definition. Integrating equation (7) and using the dimensionless bed shear stress T_b yields

$$E = M\rho_w\sigma_u^2 \int_{T_c}^{\infty} (T_b - T_c) r(T_b)\mathrm{d}T_b. \tag{8}$$

The erosion rate is now a function of the mean bed shear stress only as T_b, T_c and σ_u scale with the mean bed shear stress: $T_b = \frac{\tau_b}{\langle\tau_b\rangle(\delta^2+1)}$, $T_c = \frac{\tau_c}{\langle\tau_b\rangle(\delta^2+1)}$, and $\sigma_u^2 = (\delta^2+1)\frac{\langle\tau_b\rangle}{\rho_w}$.

[25] The form in equation (8) is similar to erosion formulations with stochastic forcing, as used for noncohesive sediments [see, e.g., *Van Rijn*, 1993]. If we consider the formulation equation (1) of *Partheniades* [1965] again, it follows from equation (8) that the time scale t^{τ_b} scales with $1/(T_b - T_c)$. We therefore assume that the time scale to dislodge a particle is inversely proportional to the difference between the bed shear stress and the critical bed shear stress. This is in line with Partheniades' hypothesis that t^{τ_b} is a function of τ_b, although he placed t^{τ_b} outside the integral. Equation (8) is also slightly different from equation (5.23b) of *Winterwerp and van Kesteren* [2004] as they did not subtract T_c, implying that the erosion scales with T_b instead of with $T_b - T_c$. Integration from T_c to ∞ implies that only bed shear stresses larger than the critical value are accounted for.

[26] Substituting equation (6) into equation (8) and using T_b^* gives

$$\frac{E}{M\rho_w\sigma_u^2} = \frac{1}{2\sqrt{2\pi}}\frac{1}{\alpha}\int_{T_c^*}^{\infty} \frac{T_b^* - T_c^*}{\sqrt{T_b^*}} \exp\left[-\frac{1}{2}\left(\sqrt{T_b^*} - \delta\right)^2\right]\mathrm{d}T_b^*, \tag{9}$$

with $T_c^* = \alpha T_c - \beta\delta^2$. The analytical solution for this integral reads (with the use of Maple v12.0)

$$\begin{aligned}\int (T_b^* - T_c^*) r(T_b^*)\mathrm{d}T_b^* = \\ - T_c^* - \frac{\sqrt{T_b^*} + \delta}{\sqrt{(2\pi)}} \exp\left(-\frac{T_b^*}{2} + \delta\sqrt{T_b^*} - \frac{\delta^2}{2}\right) \\ - \frac{1}{2}\left(\delta^2 + 1 - T_c^*\right)\mathrm{erf}\left(-\sqrt{\frac{T_b^*}{2}} + \frac{\delta}{\sqrt{2}}\right).\end{aligned} \tag{10}$$

For the given boundaries (T_c^* and ∞) the following solution is obtained for the erosion rate

$$\begin{aligned}\frac{E}{M\rho_w\sigma_u^2} = \frac{-T_c^* + \delta^2 + 1}{2\alpha} \\ + \frac{\sqrt{T_c^*} + \delta}{\alpha\sqrt{(2\pi)}} \exp\left(-\frac{T_c^*}{2} + \delta\sqrt{T_c^*} - \frac{\delta^2}{2}\right) \\ + \frac{\delta^2 + 1 - T_c^*}{2\alpha}\mathrm{erf}\left(-\sqrt{\frac{T_c^*}{2}} + \frac{\delta}{\sqrt{2}}\right).\end{aligned} \tag{11}$$

Note that the mean bed shear stress is incorporated in T_c^* and σ_u. Figure 2 shows the erosion rate of equation (11) as function of mean bed shear stress $\langle\tau_b\rangle$. Additionally, the linear formulation is shown. The graph of the improved erosion rate according to equation (11) shows a gradual initial increase and converges to the linear formulation at larger values for $\langle\tau_b\rangle$. This behavior is significantly different from

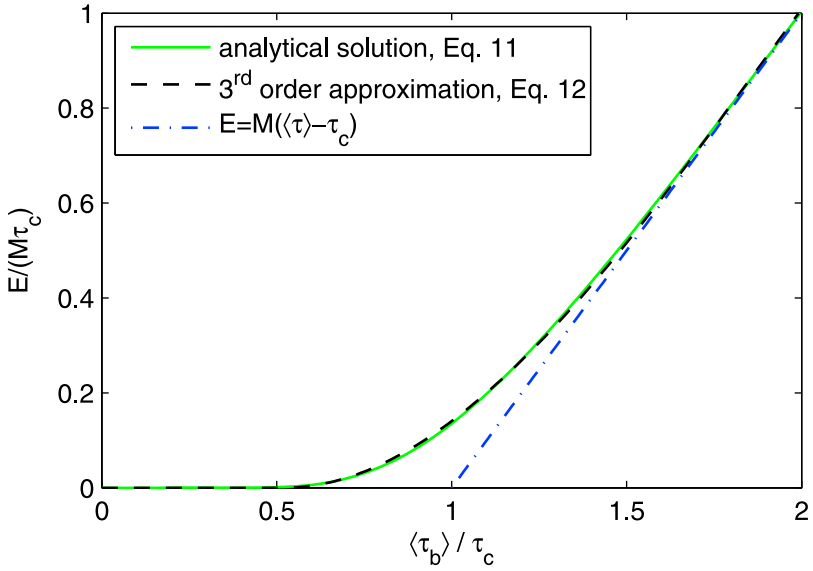

Figure 2. Erosion rates with stochastic forcing, according to the analytical formulation of equation (11), the simplified parameterization of equation (12), and the linear formulation.

the behavior of the formulation as given by *Partheniades* [1965], as plotted in the discussion on the paper of Partheniades by *Christensen* [1965]. The formulation of Partheniades tends to a constant erosion rate for large bed shear stresses, whereas our formulation tends to a linearly increasing erosion rate. This difference is the result of placing the time scale t^{τ_b} within the integral.

[27] Equation (11) is not convenient in numerical models, and therefore a simpler parameterized expression is desired. A third-order polynomial fits this function. The polynomial with the following constants reflects equation (11) with a maximum error of $\Delta E < 0.01 M\tau_c$

$$\frac{E}{M\tau_c} = \begin{cases} 0 & \text{if } \dfrac{\langle\tau_b\rangle}{\tau_c} < 0.52 \\ a_1\left(\dfrac{\langle\tau_b\rangle}{\tau_c}\right)^3 + a_2\left(\dfrac{\langle\tau_b\rangle}{\tau_c}\right)^2 + a_3\left(\dfrac{\langle\tau_b\rangle}{\tau_c}\right) + a_4 & \\ \left(\dfrac{\langle\tau_b\rangle}{\tau_c} - 1\right) & \text{if } \dfrac{\langle\tau_b\rangle}{\tau_c} > 1.7 \end{cases}, \tag{12}$$

with $a_1 = -0.144$; $a_2 = 0.904$; $a_3 = -0.823$; $a_4 = 0.204$. This parameterized expression is shown in Figure 2 as well. An erosion rate formulation (equation (12)) is obtained, based on the distribution of the bed shear stress, but expressed in terms of the mean bed shear stress.

5. Critical Bed Shear Stress Distribution

[28] In this section, we develop a stochastic description of the bed strength (critical shear stress for erosion). The erosion of noncohesive particles is determined by the weight and size of the particles and the position of the particle within the bed. In case of cohesive sediment, cohesive forces also contribute to (or dominate) the total force balance. The weight and size of the particles and the cohesive forces are generally parameterized by a critical shear stress τ_c. The position of the particle in the bed has to be taken into account by a bed model. Such a bed model is trivial in case of uniform sediment, but becomes complicated for nonuniform sediment. Commonly, the bed is discretized into a finite number of layers. A bed model widely used is the active layer approach of *Hirano* [1971]. The bed is schematized by an active layer (or exchange layer) and a lower layer (or substrate), see Figure 3. The active layer interacts with the water column by means of erosion and deposition fluxes. *Armanini* [1995] subdivided the substrate further into several sublayers, communicating by advective and diffusive fluxes. The diffusive fluxes represent physical and/or biological mixing.

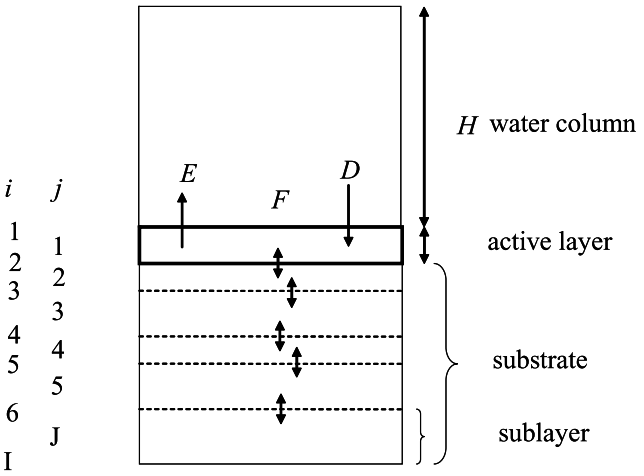

Figure 3. Schematization of the bed with an active layer and a substrate with several sublayers. Here i is a counter for interfaces and j is a counter for the layers. In the present study there is only one active layer ($j = 1$) and one single substrate layer ($j = 2$).

[29] The thickness of the active layer appears to be an important parameter. In reality, the probability of a particle to erode decreases smoothly toward zero, deeper into the bed. However, in the active layer concept this smooth transition is represented by a Dirac function; in the active layer all particles have an equal probability of erosion (the layer is well mixed), whereas in the substrate layer, sediments cannot erode.

[30] In case of noncohesive sediment, the thickness of the active layer should depend on the roughness length scales of the bed. For ripples/dunes, the ripple/dune height turns out to be an appropriate length scale $\Delta = 0.5\eta$, with ripple/dune height η [see *Blom*, 2003]. In case of plane beds, the maximum grain diameter is often used as length scale $\Delta = D_{90}$. For cohesive sediments, no data are available to define the active layer thickness. In case of plane beds, the floc diameter seems an appropriate scale. The substrate is only important as a boundary condition for the active layer; it is often subdivided into multiple layers, which is important in case of strong gradients in critical bed shear stress over the depth.

[31] To account for nonuniformity, the sediment composition is described through classes. These classes represent a distribution in critical bed shear stress. In case of noncohesive sediment, a class would relate to grain diameter. In case of cohesive sediments this is not necessarily the case, as cohesive forces play a role.

[32] The sediment balance equations for the water column and the active layer of the bed are

$$\frac{\mathrm{d}hc_n}{\mathrm{d}t} = E_n - D_n \tag{13}$$

$$\frac{\mathrm{d}m_{n,j=1}}{\mathrm{d}t} = -E_n + D_n + F_{n,i=2}, \tag{14}$$

with h the water depth, c the dry sediment mass per volume water (kg m^{-3}) for fraction n, m_j (kg m^{-2}) the specific sediment mass in layer j, E_n (kg m^{-2} s^{-1}) the erosion flux for fraction n (defined positively upward), D_n (kg m^{-2} s^{-1}) the deposition flux for fraction n (defined positively downward) and $F_{n,i=2}$ (kg m^{-2} s^{-2}) the flux of sediment through the interface ($i = 2$) between the active layer and the underlying substrate. The change in bed level (z_b) is given by

$$\frac{\mathrm{d}z_b}{\mathrm{d}t} = \frac{1}{\phi_s \rho_s}\left(\sum_{n=1}^{N} D_n - \sum_{n=1}^{N} E_n\right), \tag{15}$$

with N the number of classes, ϕ_s the volume fraction of sediment and ρ_s the dry sediment density.

[33] For each class, an erosion formulation is defined

$$E_n = p_{n,j=1} f\left(\langle \tau_b \rangle, \tau_{c,n}, M_n\right), \tag{16}$$

with $p_{n,j=1} = m_{n,j=1}/(\rho_s \phi_s \Delta_1)$ the mass fraction of sediment n in the active layer ($j = 1$) with thickness Δ_1, f the erosion function as defined in equation (11) or equation (12), $\tau_{c,n}$ the critical bed shear stress of class n and M_n the erosion rate coefficient of class n.

[34] Following *Parchure and Mehta* [1985] we neglect the deposition term ($D = 0$). In a next stage the deposition term can be elaborated. An important question reads "Do the sediment particles stay in the same class?." It is not likely that a particle that was eroded from a consolidated bed will maintain its critical bed shear stress when it deposits again. It is expected that the critical bed shear stress of the deposited sediment is much smaller. Our assumption of a negligible deposition can therefore also be interpreted by a negligible critical bed shear stress of the deposited sediment ($\tau_c = 0$). All deposited sediment directly erodes again.

[35] The flux $F_{n,i=2}$ consists of an advection part and a mixing part

$$F_{n,i=2} = \phi_s \rho_s \frac{\mathrm{d}z_b}{\mathrm{d}t} p_{n,i=2} + MIX_{i=2}. \tag{17}$$

The advection part (first term on the r.h.s) is a consequence of the combination of the use of a constant active layer thickness, and aggradation/degradation. The mixing term ($MIX_{i=2}$) at the interface ($i = 2$) between the active layer and the substrate is governed by physical mixing due to ripple migration, and by biological mixing. Although mixing is often described by a diffusion process, nondiffusive mixing may occur as well. The time scale of mixing is generally much larger than that for erosion. We therefore neglect mixing herein ($MIX_{i=2} = 0$). In a further development of the model, this can be taken into account.

[36] In the remainder, we consider the substrate as an infinitely thick single layer. The fluxes between substrate sublayers are therefore not further discussed. Subdivision of the substrate can be implemented in future to model stratified beds.

[37] In principle, the model is fully formulated by the balance equations (equation (13) and (14)) and the flux definitions (equations (16) and (17)). However, these formulations contain a number of parameters, and are therefore not directly applicable. Therefore, the following simplifications and assumptions are made:

[38] 1. The thickness of the active layer Δ is kept constant and should be of the order of the (floc)diameter, $\Delta = \mathcal{O}(\mu$m-mm). It is noted that the layer thickness may have to increase significantly to about the ripple height when bed forms are present.

[39] 2. As mentioned above, deposition and mixing between the layers are neglected.

[40] 3. The sediment volume fraction (ϕ_s) is constant. In principle the volume fraction will increase with depth due to consolidation. However, *Partheniades* [1965] and *Amos et al.* [1992a] argue that the self-weight consolidation in the top 10 mm is of minor importance. Furthermore, biological activity (e.g., *Corophium volutator*) will mix the top layer, resulting in a more homogeneous mixture. In this paper the volume fraction is kept constant, but in future, the volume fraction may be linked to the vertical position in the bed.

[41] 4. The parameter M is constant and equal for all classes, although it is expected that the erosion rate coefficient will decrease for sediment with a higher strength. A change in critical bed shear stress distribution should therefore also result in a change in M. However, to reduce the number of parameters M is kept constant.

[42] 5. To solve the set of equations, the initial distribution of the critical bed shear stress in the active layer and in the substrate has to be prescribed. The initial distribution of the active layer is assumed to be equal to the distribution of the underlying substrate. In the real world, the distribution in the active layer may deviate from the one in the lower layer due to physical, biological and chemical processes. The substrate may be stratified as well. The initial critical bed shear stress differs for each class and the distribution is assumed to be Gaussian. The strength in general, and the distribution of the strength in particular, of the top layer is difficult to measure directly. Indirect measurements can be done with flume tests. The initial truncated Gaussian distribution of the critical bed shear stress in the active layer and in the substrate is defined by

$$p(\tau_c) = \frac{1}{\sigma_{\tau_c}\sqrt{2\pi}} e^{\frac{-(\tau_{c,n}-\mu_{\tau_c})^2}{2\sigma_{\tau_c}^2}}, \qquad \tau_c > 0, \tag{18}$$

with mean value μ_{τ_c} and standard deviation σ_{τ_c} of τ_c. Both parameters have to be assessed through calibration of the model.

[43] 6. The different classes are treated separately, without mutual interaction. In nature it is well possible that the classes influence each other by, e.g., hiding effects and cohesive forces.

6. Application to Data Set of *Jacobs* [2009]

[44] The model above described is first applied to simulate an annular flume experiment carried out at Delft University of Technology by *Jacobs* [2009]. The flow in this flume is described in detail by *Booij* [2003]. The flume has a diameter of 3.7 m and a water depth of 27.4 cm. Its top lid rotates driving the flow, and the flume itself rotates in opposite direction reducing secondary circulations. A remolded, muddy sediment mixture was used, consisting of 16% clay (kaolinite), 64% silt and 20% sand. During the experiment, the velocities were increased from 0 to 0.8 m/s in steps of approximately 10 minutes. The friction velocity was determined by $u_* = \sqrt{c_f}\, U$, with friction coefficient $c_f = 0.0026$, and measured depth-mean flow velocity U. The value for the bed friction coefficient followed from numerical simulations [*Booij*, 2003]. The maximum associated bed shear stress was 1.6 Pa. Figure 4a shows the imposed velocities and associated bed shear stresses. Figure 4b shows the development of concentration in the water column as a result of bed erosion. The concentration was uniformly distributed over the water depth. The maximum concentration (at the end of the experiment) is 5 kg m^{-3}. The bulk density of the bed was approximately 1800 kg m^{-3}, uniform with depth. The average thickness of the eroded layer is then 750 μm. From the concentration time series, the erosion rates can be determined by differentiating in time. The erosion rate development is plotted in Figure 4c. As the erosion signal is noisy, a low-pass filter is applied with a window of 30 s.

[45] The erosion signal can be divided in three stages. In the first stage ($t < 30$ min), no erosion takes place. The bed shear stress is not high enough to erode the bed noticeably. In the second stage (30 min $< t <$ 90 min) the erosion rate increases sharply to a maximum, but drops again shortly after at low velocities. This stage is comparable to Type I (supply limited) erosion, and can be regarded as floc erosion. Erosion continues until the available erodible material is eroded. At larger velocities, a constant erosion rate establishes after some time. In the third stage ($t > 90$ min), the erosion rate becomes constant directly after increasing the velocity. This can be considered as Type II (unlimited) erosion.

[46] In order to model the development of the concentration in the water column during the experiment, several parameters have to be tuned. For the hydrodynamics, the parameters described in section 4 are used, resulting in erosion formulation equation (12). The bed has to be divided into a finite number of classes with an initial critical bed shear stress ($N = 50$ is chosen). Furthermore, the critical bed shear stresses of the underlying substrate have to be set. Finally, the erosion rate coefficient M and the thickness of the active layer must be defined. The parameters to be tuned are Δ, σ_{τ_c}, μ_{τ_c}, and M, to reproduce the development of the concentration and the erosion rate properly.

[47] The active layer thickness is set to $\Delta = 50$ μm. This value is within the expected range of floc diameters. The parameter M determines the adaptation time of the erosion process at the transition from one velocity step to the next. This is shown in Figure 5a. A higher value for M leads to a higher peak erosion. The decrease of the peak is also faster. M is calibrated against this decrease of the erosion rate and is set to $M = 0.009$ s m^{-1}. Increasing parameter σ_{τ_c} leads to a significantly steeper overall curve, see Figure 5b. Multiplying σ_{τ_c} by 0.5 leads to an increase in erosion rate at the highest velocity with a factor 9. The steepness of the overall curve is tuned with $\sigma_{\tau_c} = 1.30$ Pa. The results are less sensitive to μ_{τ_c}, as shown in Figure 5c, and its value is set to $\mu_{\tau_c} = 0.40$ Pa. These values imply a truncated Gaussian distribution; μ_{τ_c} is therefore not the mean value. The mean value is 1 Pa, which is approximately the bed shear stress at which the erosion rates become constant. The initial critical bed shear stress distribution, thus obtained, is shown in Figure 6.

[48] The computed concentration c (coefficient of determination $R^2 = 0.998$) and erosion rate E ($R^2 = 0.955$) are plotted against time in Figures 4b and 4c. As the concentration c is a cumulative variable, errors initiated at the early stage of the experiment are still present in later stages. It is therefore more appropriate to consider the erosion rate E in Figure 4c. The first three peaks in the measured erosion rate diagram are poorly reproduced. This might be caused by an incorrect initial PDF of the critical bed shear stress of the active layer due to, e.g., loose particles on the bed. Among other factors, initial bed irregularities may play a role. Acceleration effects, occurring when the velocity changes from one step to the other, may also be of importance. Note that changing the parameters does not result in higher peaks during the first velocity steps, see Figure 5. For the calibration, the parameters were tuned to the period $t > 60$ min, as at that time most of the erosion took place. Until $t = 90$ min, the measured erosion rate decreases exponentially after its initial increase in response to an increase in velocity. The erosion steps were however too short to determine if the erosion rate would reduce to zero for 60 min $< t <$ 80 min. For $t > 85$ min, the erosion rate stays more or less constant, indicating the transition from Type I (supply limited) to Type II (unlimited) erosion. Constant erosion rates are found for the last two

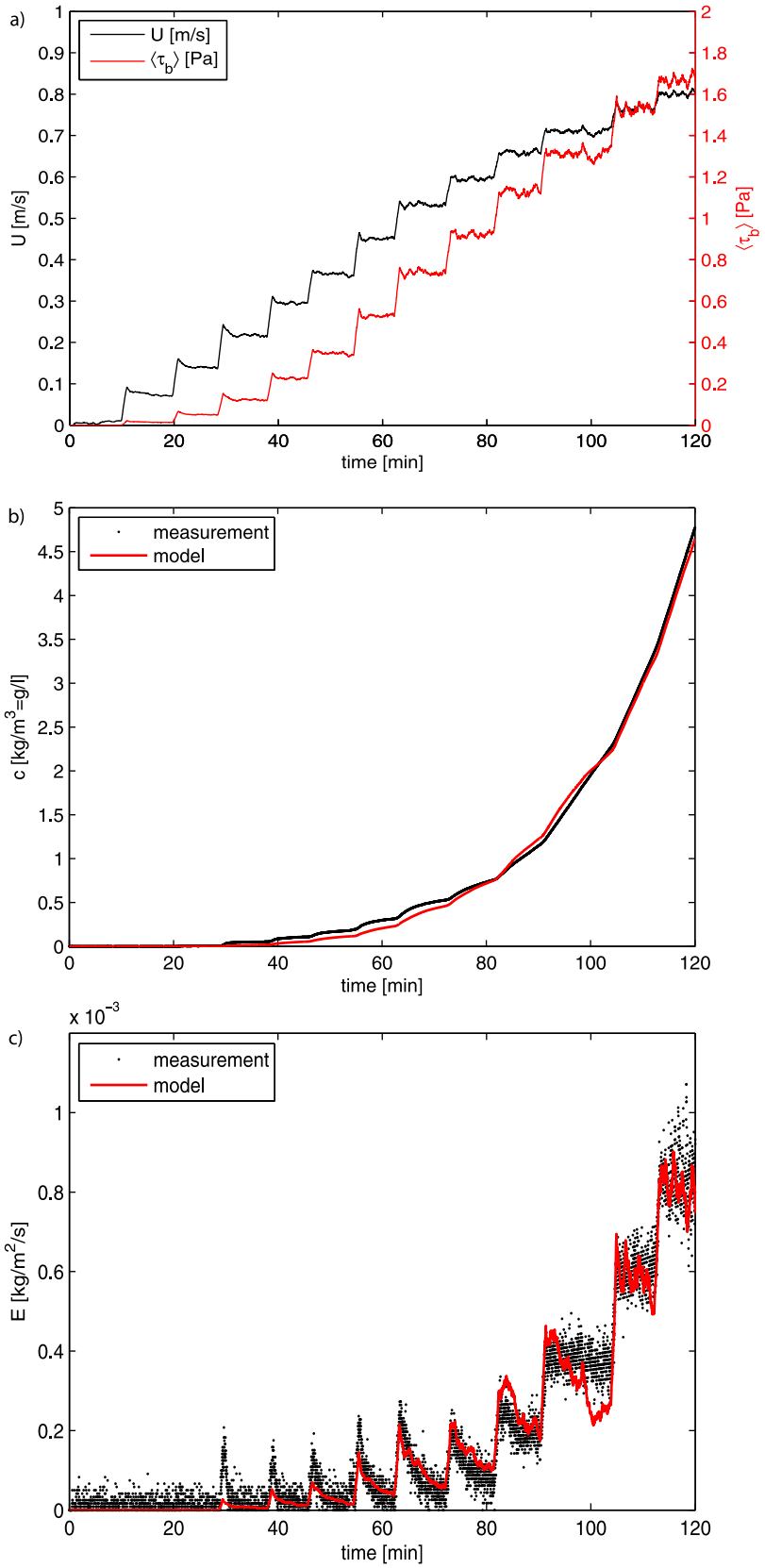

Figure 4. (a) Measured velocity and associated bed shear stress in time. (b) Measured and computed concentration in time. (c) Measured and computed erosion rate in time. Results are low-pass filtered with a window of 30 s. Laboratory measurements are from *Jacobs* [2009].

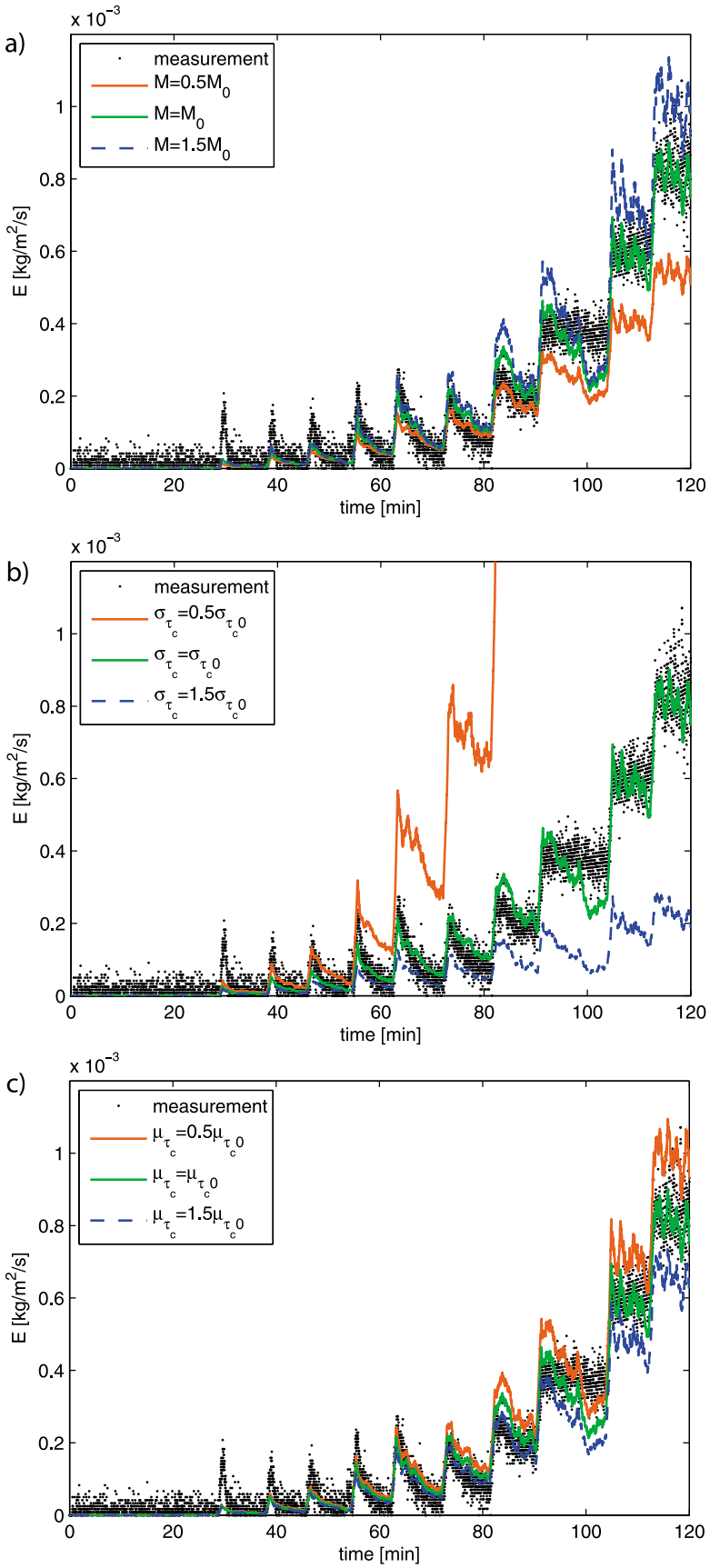

Figure 5. Sensitivity of erosion rate (E) to the parameters (a) M, (b) σ_τ, and (c) μ_τ. The calibrated values, indicated with subscript 0, are multiplied with factors 0.5, 1, and 1.5. Laboratory measurements are from *Jacobs* [2009].

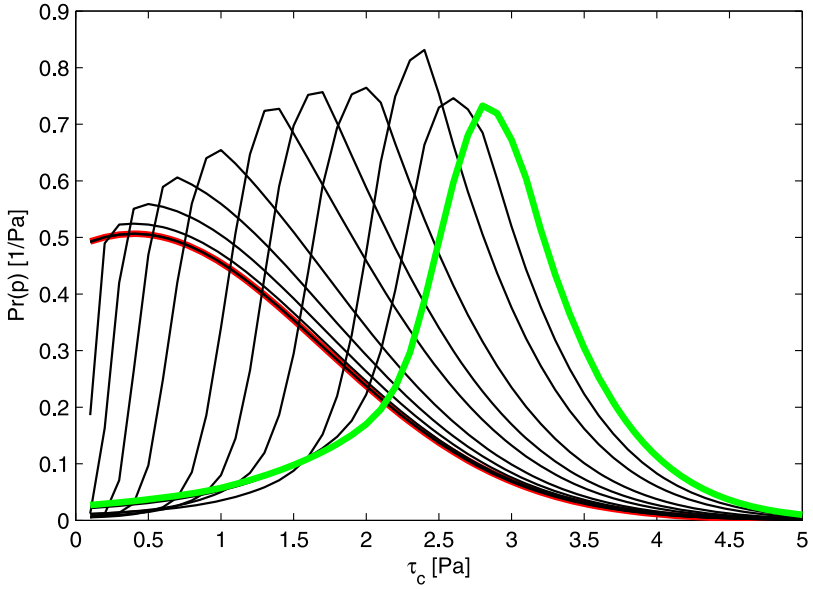

Figure 6. Development of the distribution of the critical bed shear stress in the bed at the end of each erosion step. Red line indicates initial distribution and the distribution of the underlying substrate. Green line indicates final distribution.

steps. The computed equilibrium values of the erosion rate for $t > 105$ min are close to the measurements.

[49] The development of the critical bed shear stress distribution in time is shown in Figure 6. This is the critical bed shear stress of the particles at the moment they were eroded. When these deposit again, the critical bed shear stress will be lower. With increasing flow velocity, the mean critical bed shear stress increases. The easily erodible sediment vanishes rapidly, and stronger fractions remain in the bed. Note that this increase of the critical bed shear stress is similar to the findings of, e.g., *Parchure and Mehta* [1985] or *Amos et al.* [1992a]. However, they attributed the increase in critical shear stress to an increase of the strength over the depth. As mentioned earlier, this is plausible for freshly deposited beds, but arguable for denser beds.

[50] The development of the distribution of the concentration in the water is shown in Figure 7. Note that particles in suspension cannot have a critical bed shear stress. The plotted distribution represents the distribution at the moment when the particles were dislodged from the bed. There is a significant difference between the distribution of the sediment in the water and in the bed. The water column contains sediments which were easily eroded, whereas the sediments hard to erode, stay in the bed. As soon as a part of the bed erodes,

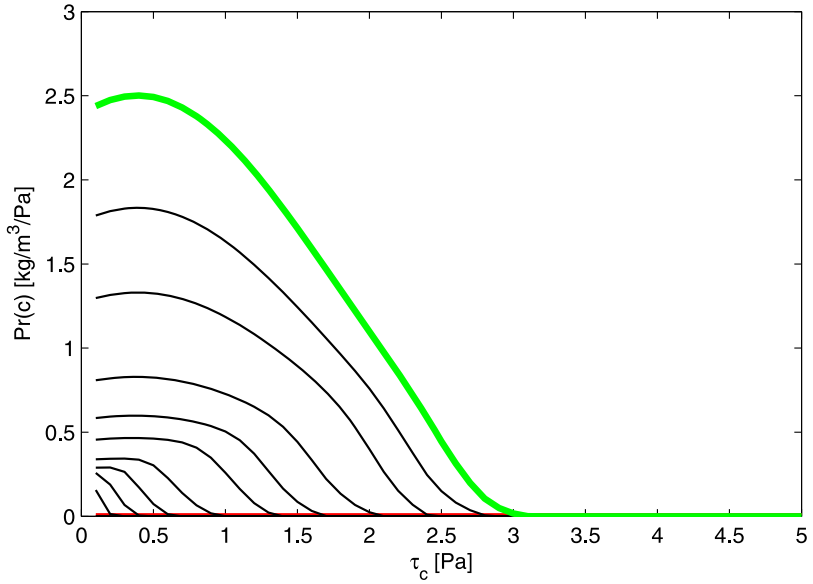

Figure 7. Development of the distribution of the classes of critical bed shear stress in the water column at the end of each erosion step. Red line indicates initial distribution and the green line indicates final distribution.

the underlying easily erodible material almost directly entrains into the water column.

[51] The release of sediments with a low critical bed shear stress and the subsequent increase of the mean critical bed shear stress of the bed is very similar to the winnowing of fine sediments from a coarse sediment bed as found in found in field observations and other models [*Wiberg et al.*, 1994; *Harris and Wiberg*, 2001; *Law et al.*, 2008]. In our case, however, it is difficult to identify the class of the particle via direct measurements, as the class is not only related to the particle size, but also to the cohesiveness of the bed. The class is therefore not only a particle property, but also a bed property.

7. Application to the Data of *Amos et al.* [1992a]

[52] *Amos et al.* [1992a] carried out field measurements with the Sea Carousel in the Bay of Fundy. The Sea Carousel is an annular flume with a diameter of 2 m as described by *Amos et al.* [1992a]. Here, we model the data from Figure 3a of *Amos et al.* [1992a]. The measured velocity is digitized and used as input, see Figure 8a. This velocity has to be translated into a bed shear stress. The bed shear stress is defined by $\langle \tau_b \rangle = \rho_w c_f U^2$ with an estimated friction coefficient of $c_f = 0.0025$.

[53] A trial and error approach similar to section 6 was followed to obtain the various parameters and we found $\Delta = 30$ μm, $M = 0.020$ s/m, $\mu_{\tau_c} = 0.39$ Pa and $\sigma_{\tau_c} = 1.28$ Pa. These values are close to the values found for the set of *Jacobs* [2009], $\Delta = 50$ μm, $M = 0.009$ s/m, $\mu_{\tau_c} = 0.40$ Pa and $\sigma_{\tau_c} = 1.3$ Pa. The resulting concentration evolution is shown in Figure 8b. The computed results are in good agreement with the measurements (the lower curve of the measurements SSC1 in Figure 8b was aimed at). The erosion rates are plotted in Figure 8c. In tandem with the concentration development, these results are close to the measured results as well.

[54] The used friction coefficient is smaller than the value proposed by *Amos et al.* [1992b], $c_f = 0.015$, which is similar to a Chézy value of $C = 26$ m$^{1/2}$ s^{-1}. This friction coefficient is relatively high. Exactly the same concentration and erosion rate evolution can be obtained with a different value for c_f, as the parameters μ_τ, σ_τ and M scale linearly with c_f. Multiplying c_f by 6 requires multiplying μ_τ and σ_τ by 6 and dividing M by 6. The resulting values are then, $M = 0.0034$ s/m, $\mu_{\tau_c} = 2.35$ Pa and $\sigma_{\tau_c} = 7.7$ Pa. The values for the critical bed shear stress turn out to be very high. We therefore proposed the more realistic value for the friction coefficient as given at the beginning of this section.

[55] Also the experiments of *Amos et al.* [1992a] can be simulated rather well with the proposed modeling concept with constant parameters Δ, M, μ_{τ_c} and σ_{τ_c}. This gives confidence for the proposed modeling concept and the assumptions made.

8. Discussion and Conclusions

[56] Our first aim was to simulate incipient motion of cohesive sediment beds exposed to turbulent flow. Therefore, turbulent fluctuations of the bed shear stress were taken into account, using the distribution of *Hofland and Battjes* [2006]. However, this formulation did not reproduce the standard deviation properly. Though, a modification yields good resemblance of measured bed shear stress distributions, but we have no physical arguments for this modification. The parameters are tuned for relatively low Reynolds number, uniform flows with a hydraulically smooth bed. Although there are no direct indications that the parameters will change for high Reynolds number flows or for rough beds, we could not validate this, as no measurements are available. The bed shear stress distribution was implemented in the linear erosion rate formulation. A complicated erosion formulation was obtained, which was simplified to a third-order polynomial. This erosion formulation only depends on the mean bed shear stress.

[57] There is no sound physical explanation for the linear relation, which is based on fits through data of erosion rates for $\tau_b > \tau_c$. For example, note that the erosion rate for sand is often of the form $E = A(\tau_b - \tau_c)^{3/2}$ [*Fernandez Luque and Van Beek*, 1976; *Van Rijn*, 1984]. Yet, also for this noncohesive transport no sound physical explanation is known for the exponent 3/2 [see, e.g., *Parker et al.*, 2003]. In principle, the new relation is therefore not much better than an arbitrary type of function that fits the data of, e.g., *Partheniades* [1965]. The advantages of the newly derived erosion rate formulation are, however, (1) it is consistent with the linear relation for $\tau_b \gg \tau_c$ and therefore with many measurements and (2) the formulation takes into account the distribution of the turbulence levels near the bed. In principle, other types of flow, such as accelerating or decelerating flows with another ratio δ between the mean flow and the fluctuations can be simulated as well [see *Hofland and Battjes*, 2006]. However, not only the stochastic forcing influences the incipient motion, but also the nonuniformity of the bed partly determines the erosion rate at low bed shear stresses.

[58] Our second aim was to analyze and simulate the time dependency (or supply dependency) of observed erosion rates. Our approach with a nonuniform critical bed shear stress is an alternative to the approach with stratified beds as proposed by *Sanford and Maa* [2001]. Based on the measurements, it is not possible to decide whether the time-dependent behavior is caused by stratification of the bed, or by nonuniformity of the sediment. Both concepts yield initial erosion of easily erodible (fine) sediment, both yield a tendency of the erosion rate to zero for small shear stresses, and both yield a constant erosion rate for high shear stresses. Note that this only holds for stratified beds, for which the critical bed shear stress increases with depth. For soft beds, as studied by *Mehta and Partheniades* [1982], the stratification of the bed density strongly suggests that time-dependent behavior is due to this stratification. For the denser beds, the eroded layer in most experiments is smaller than 1 mm, our approach with a nonuniform bed seems more appropriate. Detailed measurements within the bed are required however to determine which concept is most plausible. From a practical point of view, there is little difference between the two concepts. Both can therefore be applied. Note that a stratified bed can also be accounted for in the proposed stochastic approach. In that case, the substrate has to be subdivided into sublayers with different distributions for the critical bed shear stress.

[59] The model performs well for the two annular flume data sets. However, calibration had to be carried out by trial and error. The effects of varying the parameters are somewhat

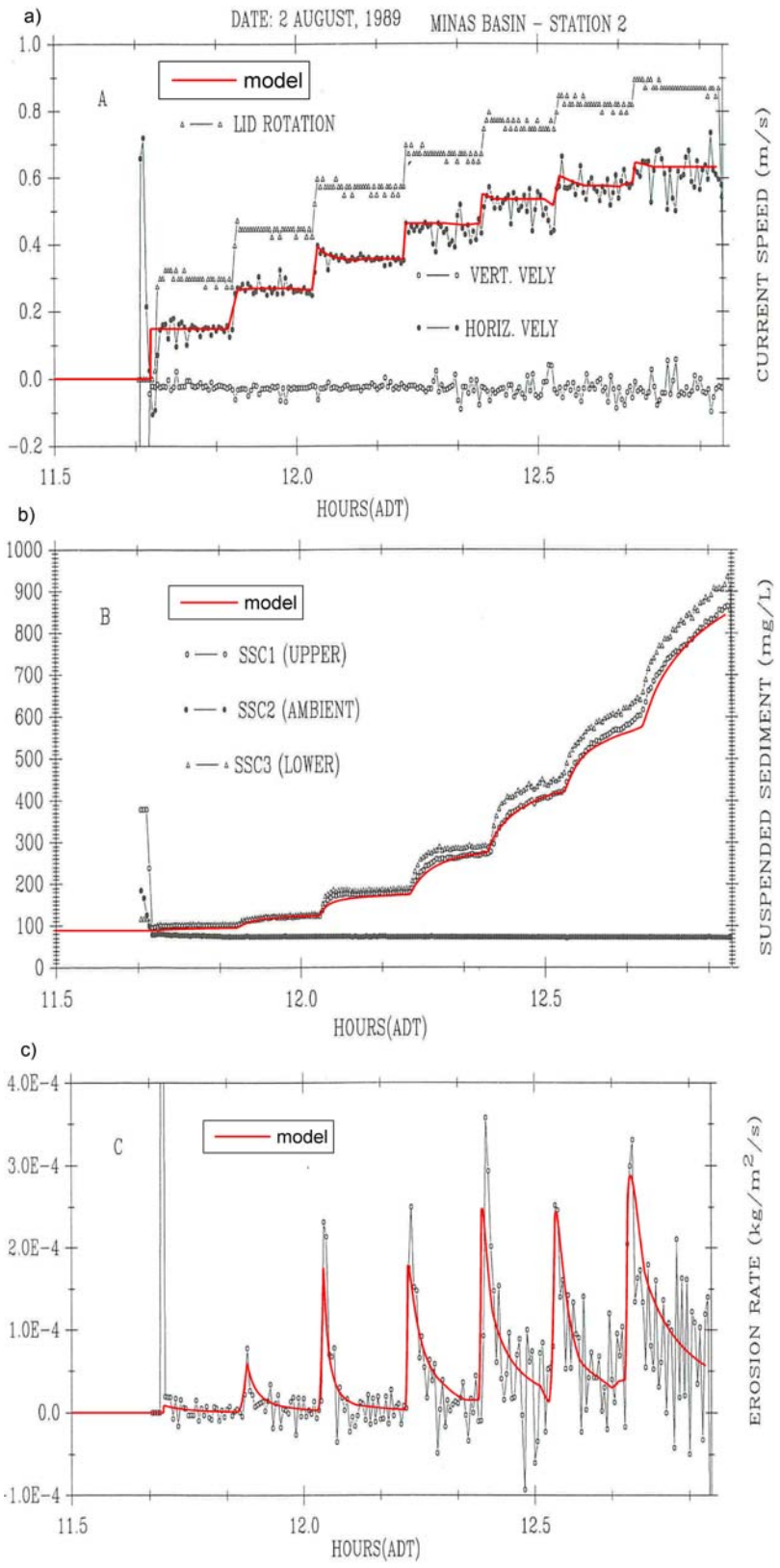

Figure 8. (a) Measured velocity with time with digitized velocity as used in the model. (b) Measured and computed concentrations with time. (c) Measured and computed erosion rates with time. Original figures from *Amos et al.* [1992a], reprinted with permission from Elsevier.

correlated. In other words, the change of one parameter can partly be compensated by tuning one of the others. It would be valuable if the parameters could be determined fully independently, but our physical understanding of the erosion process is still too limited. The thickness of the active layer may possibly be determined by careful video observations, or experiments with tracer particles. The distribution of the strength of the bed is hard to determine directly. To the authors' knowledge there are no instruments available to measure (the distribution of) the strength at the scale of μm mm. The coefficient M is a calibration coefficient. In this study, M is kept constant for all classes. However, it is possible that M and τ_c are related. Furthermore, M may be depth dependent as suggested by *Sanford and Maa* [2001]. The distribution of the critical bed shear stress and the erosion coefficient have to be determined indirectly from flume experiments or likewise. Calibration of the model against other data sets, containing time series of erosion rates, is desired to obtain better insights in the range of the parameters.

[60] In this paper we consider the erosion process for fine cohesive sediments only. We assume that deposition can be neglected for the laboratory experiments, following *Parchure and Mehta* [1985]. In reality, deposition will play a role, especially on intertidal flats where velocities can drop to zero. Technically, it is simple to include a deposition term in the proposed model. However, it will be a difficult task to determine the critical bed shear stress of the freshly deposited sediment. It is not likely that a particle that was eroded from a consolidated bed will maintain its critical bed shear stress when it deposits again. It is expected that the critical bed shear stress is much smaller. Our assumption of a negligible deposition can therefore also be interpreted by a negligible critical bed shear stress of the deposited sediment ($\tau_c = 0$). All deposited sediment directly erodes again. Further study is required to validate this hypothesis. Deposition will also play a role when the bed is mixed with coarse sediment. In that case, the hypothesis of exclusive erosion *Parchure and Mehta* [1985] will certainly not hold anymore.

[61] For natural conditions, the parameters and initial conditions will strongly depend on biological and chemical processes as well. For example, diatom mats will influence the critical bed shear stress of the active layer and *Hydrobia ulvae* destabilizes the top layer by their tracks. These processes may be accounted for in the presented framework, not only by changing M, but also by a change in distribution of τ_c. A first attempt has been made by *Van Prooijen and Montserrat* [2009] by including the effect of the invertebrate Macoma balthica on the erosion rate. Evidently, these relations have to be explored in more detail.

[62] **Acknowledgments.** This research was supported by the Technology Foundation STW, Applied Science Division of NWO, and the technology programme of the Ministry of Economic Affairs. The authors thank an anonymous reviewer for constructive comments. Furthermore, we thank Mehta for his comments on the manuscript. Finally, we highly appreciate that Walter Jacobs provided his experimental results and shared his knowledge on this topic.

References

Aberle, J., V. Nikora, S. McLean, C. Doscher, I. McEwan, M. Green, D. Goring, and J. Walsh (2003), Straight benthic flow-through flume for in situ measurement of cohesive sediment dynamics, *J. Hydraul. Eng.*, *129*(1), 63–67.

Amos, C. L., G. R. Daborn, H. A. Christian, A. Atkinson, and A. Robertson (1992a), In situ erosion measurements on fine-grained sediments from the Bay of Fundy, *Mar. Geol.*, *108*, 175–196.

Amos, C. L., J. Grant, G. R. Daborn, and K. Black (1992b), Sea Carousel: A benthic, annular flume, *Estuarine Coastal Shelf Sci.*, *34*(6), 557–577.

Armanini, A. (1995), Non-uniform sediment transport: Dynamics of the active layer, *J. Hydraul. Res.*, *33*(5), 611–622.

Blom, A. (2003), A vertical sorting model for rivers with non-uniform sediment and dunes, Ph.D. thesis, Univ. of Twente, Enschede, Netherlands.

Booij, R. (2003), Measurements and large eddy simulations of the flows in some curved flumes, *J. Turbulence*, *4*, 8.

Christensen, B. A. (1965), Discussion on "Erosion and deposition of cohesive soils," *J. Hydraul. Div. Am. Soc. Civ. Eng.*, *9*(5), 301–308.

De Ruiter, J. (1982), The mechanism of sediment transport on bedforms, in *Euromech 156: Mechanics of Sediment Transport*, edited by B. Sumer and A. Muller, pp. 137–142, Balkema, Rotterdam, Netherlands.

Einstein, H. A. (1950), The bedload function for sediment transportation in open channels, *Tech. Bull. 1026*, U.S. Dep. of Agric., Washington, D. C.

Fernandez Luque, R., and R. van Beek (1976), Erosion and transport of bed-load sediment, *J. Hydraul. Res.*, *14*(2), 127–144.

Harris, C. K., and P. L. Wiberg (2001), A two-dimensional, time-dependent model of suspended sediment transport and bed reworking for continental shelves, *Comput. Geosci.*, *27*(6), 675–690.

Hirano, M. (1971), River bed degradation with armouring, *Proc. Jpn. Soc. Civ. Eng.*, *195*, 55–65.

Hofland, B., and J. A. Battjes (2006), Probability density function of instantaneous drag forces and shear stresses on a bed, *J. Hydraul. Eng.*, *132*(11), 1169–1175.

Jacobs, W. (2009), Erosion of sand-mud mixtures, Ph.D. thesis, Delft Univ. of Technol., Delft, Netherlands, in press.

Kandiah, A. (1974), Fundamental aspects of surface erosion of cohesive soils, Ph.D. thesis, Univ. of Calif., Davis, Calif.

Kim, J., P. Moin, and R. Moser (1987), Turbulence statistics in fully developed channel flow at low Reynolds number, *J. Fluid Mech.*, *177*, 133–166.

Krone, R. B. (1999), Effects of bed structure on erosion of cohesive sediments, *J. Hydraul. Eng.*, *125*(12), 1297–1301.

Kuijper, C., J. M. Cornelisse, and J. C. Winterwerp (1989), Research on erosive properties of cohesive sediments, *J. Geophys. Res.*, *94*, 14,341–14,350.

Law, B. A., P. S. Hill, T. G. Milligan, K. J. Curran, P. L. Wiberg, and R. A. Wheatcroft (2008), Size sorting of fine-grained sediments during erosion: Results from the western Gulf of Lions, *Cont. Shelf Res.*, *28*(15), 1935–1946, doi:10.1016/j.csr.2007.11.006.

Le Hir, P., P. Cann, B. Waeles, H. Jestin, and P. Bassoullet (2005), Erodability of natural sediments: Experiments on sand/mud mixtures from laboratory and field erosion tests, in *Sediment and Ecohydraulics: Intercoh 2005*, *Proc. Mar. Sci. Ser.*, vol. 9, edited by T. Kusuda et al., pp. 137–154, Elsevier, Amsterdam.

Le Hir, P., Y. Monbet, and F. Orvain (2007), Sediment erodability in sediment transport modeling: Can we account for biota effects?, *Cont. Shelf Res.*, *27*, 1116–1142.

Lick, W. J. (2009), *Sediment and Contaminant Transport in Surface Waters*, CRC Press, Boca Raton, Fla.

Maa, J. P. Y., L. Sanford, and J. P. Halka (1998), Sediment resuspension characteristics in Baltimore Harbor, Maryland, *Mar. Geol.*, *146*(1–4), 137–145.

McAnally, W. H., and A. J. Mehta (Eds.) (2001), *Coastal and Estuarine Fine Sediment Processes*, *Proc. Mar. Sci.*, vol. 3, Elsevier, Amsterdam.

Mehta, A. J., and E. Partheniades (1982), Resuspension of deposited cohesive sediment beds, paper presented at 18th International Conference on Coastal Engineering, Coastal Engineering Research Council, Cape Town, South Africa.

Miyagi, N., M. Kimura, H. Shoji, A. Saima, C. Ho, S. Tung, and Y. Tai (2000), Statistical analysis on wall shear stress of turbulent boundary layer in a channel flow using micro-shear stress imager, *Int. J. Heat Fluid Flow*, *21*, 576–581.

Obi, S., K. Inoue, T. Furukawa, and S. Masuda (1996), Experimental study on the statistics of wall shear stress inturbulent channel flows, *Int. J. Heat Fluid Flow*, *17*(3), 187–192.

Orvain, F., P. le Hir, and P. G. Sauriau (2003), A model of fluff layer erosion and subsequent bed erosion in the presence of the bioturbator, *Hydrobia ulvae*, *J. Mar. Res.*, *61*, 823–851.

Parchure, T. M., and A. J. Mehta (1985), Erosion of soft cohesive sediment deposits, *J. Hydraul. Eng.*, *111*(10), 1308–1326.

Parker, G., G. Seminara, and L. Solari (2003), Bed load at low Shields stress on arbitrarily sloping beds: Alternative entrainment formulation, *Water Resour. Res.*, *39*(7), 1183, doi:10.1029/2001WR001253.

Partheniades, E. (1965), Erosion and deposition of cohesive soils, *J. Hydraul. Div. Am. Soc. Civ. Eng.*, *91*, 105–139.

Partheniades, E., and R. E. Paaswell (1970), Erodibility of channels with cohesive boundary, *J. Hydraul. Div. Am. Soc. Civ. Eng.*, *96*, 755–771.

Pritchard, D., and A. J. Hogg (2003), Cross-shore sediment transport and the equilibrium morphology of mudflats under tidal currents, *J. Geophys. Res.*, *108*(C10), 3313, doi:10.1029/2002JC001570.

Roberts, J., R. Jepsen, D. Gotthard, and W. Lick (1998), Effects of particles size and bulk density on erosion of quartz particles, *J. Hydraul. Eng.*, *124*(12), 1261–1267.

Ruedi, J. D., H. Nagib, J. Osterlund, and P. A. Monkewitz (2004), Unsteady wall-shear measurements in turbulent boundary layers using MEMS, *Exp. Fluids*, *36*(3), 393–398, doi:10.1007/s00348-003-0666-1.

Sanford, L. P. (2008), Modeling a dynamically varying mixed sediment bed with erosion, deposition, bioturbation, consolidation, and armoring, *Comput. Geosci.*, *34*(10), 1263–1283, doi:10.1016/j.cageo.2008.02.011.

Sanford, L. P., and J. P. Y. Maa (2001), A unified erosion formulation for fine sediments, *Mar. Geol.*, *179*(1–2), 9–23.

Stanev, E. V., G. Brink-Spalink, and J. O. Wolff (2007), Sediment dynamics in tidally dominated environments controlled by transport and turbulence: A case study for the East Frisian Wadden Sea, *J. Geophys. Res.*, *112*, C04018, doi:10.1029/2005JC003045.

Tolhurst, T. J., K. S. Black, S. A. Shayler, S. Mather, I. Black, K. Baker, and D. M. Paterson (1999), Measuring the in situ erosion shear stress of intertidal sediments with the cohesive strength meter (csm), *Estuarine Coastal Shelf Sci.*, *49*, 281–294.

Van Ledden, M., Z. B. Wang, H. Winterwerp, and H. de Vriend (2004), Sand-mud morphodynamics in a short tidal basin, *Ocean Dyn.*, *54*(3–4), 385–391, doi:10.1007/s10236-003-0050-y.

Van Prooijen, B. C., and F. Montserrat (2009), Modeling the erosion of *Macoma balthica* affected mud beds, in *River, Coastal and Estuarine Morphodynamics*, edited by C. Vionnet et al., pp. 541–547, Taylor and Francis, London.

Van Rijn, L. (1984), Sediment pick-up functions, *J. Hydraul. Eng.*, *110*(10), 1494–1502.

Van Rijn, L. (1993), *Principles of Sediment Transport*, Aqua, Amsterdam.

Wiberg, P. L., D. E. Drake, and D. A. Cacchione (1994), Sediment resuspension and bed armoring during high bottom stress events on the northern California inner continental-shelf: Measurements and predictions, *Cont. Shelf Res.*, *14*(10–11), 1191–1219.

Widdows, J., M. D. Brinsley, N. Bowley, and C. Barrett (1998), A benthic annular flume for in situ measurement of suspension feeding/biodeposition rates and erosion potential of intertidal cohesive sediments, *Estuarine Coastal Shelf Sci.*, *46*(1), 27–38, doi:10.1006/ecss.1997.0259.

Willows, R. I., J. Widdows, and R. G. Wood (1998), Influence of an infaunal bivalve on the erosion of an intertidal cohesive sediment: A flume and modeling study, *Limnol. Oceanogr.*, *43*, 1332–1343.

Winterwerp, J. C., and W. G. M. van Kesteren (2004), *Introduction to the Physics of Cohesive Sediment in the Marine Environment*, Elsevier, Amsterdam.

B. C. Van Prooijen, Hydraulic Engineering Section, Department of Civil Engineering, Delft University of Technology, Stevinweg 1, NL-2628 CN Delft, Netherlands. (b.c.vanprooijen@tudelft.nl)

J. C. Winterwerp, Environmental Fluid Mechanics Section, Department of Civil Engineering, Delft University of Technology, Stevinweg 1, NL-2628 CN Delft, Netherlands. (j.c.winterwerp@tudelft.nl)